SORA 2.0: Stratospheric Organism and Radiation Analyzer

S. A. Garcia Morelos,[1] F. Brooks,[1] S. Oliver,[1] A. Walker,[2] K. D. Portillo,[2] R. B. Masek,[1] J. Patel,[1] S. George,[1] I. Wilson,[3] D. Pattison,[3] P. Gunaratne,[3] and A. L. Renshaw[1]

[1]*Department of Physics, University of Houston, Houston, TX, 77024, USA*

[2]*Department of Computer Science, University of Houston, Houston, TX, 77024, USA*

[3]*Department of Biology and Biochemistry, University of Houston, Houston, TX, 77024, USA*

Abstract

The SORA 2.0 payload once again sampled for the existence of microorganisms, bacterial spores and surrounding radiation in the upper atmosphere. This mission built upon the first SORA prototype [2] in order to confirm previous findings using a more developed system. The mission had three main scientific objectives. First, it built upon a further developed and novel system for isolating surrounding air. Second, an on-board MiniPIX USB particle detector analyzed real-time exposure to cosmic radiation and attempted to measure neutrons with a coupled, boron loaded scintillator. Finally, a matured version of a flight computer monitored all the systems, downlinked real-time data, and controlled all uplink commands. The payload design took advantage of additive manufacturing and hobby electronics in its construction to provide an accessible basis for future missions and explore the bounds of the technology available. SORA 2.0 returned safely and the astrobiology results pending further analysis. The MiniPIX gathered a wealth of information, with a total of 16,376 frames collected during flight. The radiation data is still being analyzed.

CONTENTS

1. MISSION AND OBJECTIVES

FIG. 1. Payload on the flightline

Braving through inclement weather, SORA 2.0 took off early on September 4, 2018 at 14:03 UTC along with 12 student payloads. From Ft. Sumner Municipal Airport, the payloads flew for approximately 9 hours. The flight terminated at 1:31 UTC the same day and then landed shortly after at 2:11 UTC about 60 miles southwest of Mt Graham, Arizona.

TABLE I. Flight information from NASA [1]

FLIGHT NUMBER:	688N
LAUNCH TIME:	09/04/2018 14:03:22 UTC
LAUNCH LOCATION:	34.473162N 104.242232W
FLOAT START:	16:30:48 UTC
TERMINATION:	09/05/2018 01:31:23 UTC
FLOAT TIME:	09:00:35
IMPACT:	02:11 UTC
IMPACT LOCATION:	32.44816666N 109.5093472W which is 60 miles SW of Mt Graham, Arizona

SORA 2.0 was a continuation flight to further develop and build upon the first SORA flight [2]. SORA's first flight in 2017 collected valuable information, yet another mission was necessary to confirm and add to the findings of the first SORA flight. Once again SORA attempted to collect extremophile bacteria and spores that may reside 36 to 41 kilometers in the upper atmosphere. For the radiation portion of SORA 2.0, a MiniPIX particle detector inside a custom built casing and coupled with a boron loaded scintillator was also flown. This was to further study the surrounding radiation and attempt to measure neutrons in order to understand the possible effects on extremophiles.

Scientific Questions

The goals and objectives for SORA 2.0 are based on the following scientific questions:

- After confirming that microorganisms are present in the upper atmosphere in the first SORA mission, what extremophiles are present in the upper atmosphere at altitudes of 36 to 41 km?

• Can Fluropore membrane filters (0.22 µm) passively capture microorganisms and spores in the upper atmosphere?

• Are the new background control protocols sufficient to confirm microorganism and spore capture?

• Coupling a boron loaded scintillator to the MiniPIX, can it detect and measure neutrons?

• If there is a measured difference in the MiniPIX due to a neutron event, is that due to the scintillator?

• Finally, with a deeper understanding of the MiniPIX after the first SORA mission, can SORA 2.0 collect more data to study cosmic radiation that microoganisms and spores experience on a daily basis? Specifically, can SORA 2.0 obtain useful information about the biological effectiveness of this radiation on bacteria through parameters such as linear energy transfer and dose equivalent?

Primary Objectives:

1. Using a refined astrobiology system, attempt to capture bacteria in the upper atmosphere at approximately 30 km to 41 km of altitude.
2. Conduct RNA analysis on samples
3. Study the cosmic and background radiation that extremophiles may experience

Secondary Objectives:

1. Couple a boron loaded scintillator to half the MiniPIX detector and attempt to measure neutrons.
2. Develop and simplify a radiation and payload flight control system.
3. Further testing of the astrobiology hardware in flight and the methodology for collection of microbes in extreme environments at high-altitude.
4. Improve pre and post-flight decontamination procedures.
5. Implement improved background control procedures.
6. Implement a variable shutter time for the MiniPIX based on the flux of particles incident on the detector.
7. Analyze the MiniPIX data in real time and downlink relevant radiation statistics.
8. Implement a redundant data storage mechanism.
9. Test an improved enclosure against impacts and harsh environments.
10. Reduce astrobiology collection apparatus size.

1.1. Hypothesis and Objectives

1. Based on the collection results from previous HASP payloads we predict the concentration of cells at an altitude of 36 km will be less than 1000 cells/L.
   (a) Objective: Sample a minimum volumetric amount of air at target altitude for the duration of the float phase (approximately 15 to 18 hours).
   (b) Status: Our pump was fully functional for the duration of the flight; thus we were able to sample a minimum volumetric amount of air at the target altitude.
2. Based on control samples and testing before flight, we can compare our final flight results to previous applications.

(a) Objective: Quantify and characterize any contamination with our laboratory and payload disinfection procedures.

(b) Objective: Minimize the amount of external contamination before flight with thorough decontamination procedures.

(c) Status: The later portion of the RNA sequencing procedures has been put on hold pending further collaboration with Qiagen field representatives.

3. Based on previous MiniPIX data, we can compare it to the current flight and observe a stark difference due to capture neutron events.

(a) Objective: Couple a boron loaded scintillator to half the MiniPIX detector for the SORA 2.0 flight.

(b) Status: Although the data has been received, it is still under analysis. The team is currently trying to better understand how the scintillator may have affected the results.

1.2. Astrobiology

Extremophiles are microorganisms that thrive in physically and/or chemically extreme conditions in which most life cannot survive. These organisms and microbes have been found everywhere, from deep underwater volcano vents to buried ice lakes in Antarctica [3]. Fungi and bacterial spores have also been found in the stratosphere. Today, the most common altitudes for organism and microbe collection in the atmosphere are in the range of approximately 10 km to 20 km above Earth's surface. Very little data exists on microbiological samples captured in the stratosphere [2]. Conditions at altitudes of 30km to 40km are extreme in temperature, pressure and radiation exposure. Arguably, each successful collection expedition, of at least 30 km into the upper atmosphere, provides information that can be useful in determining what life forms can exist inside and outside of Earth's biosphere. Additionally, RNA analysis of the organisms and microbes can provide useful insight pertaining to their ability to survive in an environment with elevated levels of radiation.

This year our experiment focused on designing a more compact collection apparatus and refining our sanitation procedures for preflight assembly, post flight disassembly, and RNA sequencing preparation. The samples we collected play an important role in expanding our knowledge about Earth's biosphere. Future studies could produce meaningful contributions to the fields of gene therapy, RNA interface, and cosmic shielding; and provide valuable insight about how life can be distributed on Earth, and ultimately, through outer-space.

1.3. Radiation

Galactic cosmic rays (GCRs) are primary particles produced outside of the solar system [4]. By colliding with other particles in Earth's atmosphere, GCRs can induce air showers consisting of secondary particles, which can be detected using sophisticated equipment. These secondary particles can be measured, thus revealing information regarding the primary particle such as energy and direction.

The mean secondary particle density reaches a peak at an altitude of about 20 km [5]. This is known as the Regener-Pfotzer Maximum, and the altitude is dependent on several environmental factors. However, when considering an individual air shower, the shower peak is greatly influenced by the initial energy of the primary particle. In cases of ultra-high energy particles, the shower maximum χ_{max} can be as low as 3 km above the Earth's surface [7]. In terms of the SORA payload, this means that the certain data, such as hits per second and dose, will reach a peak around the Regener-Pfotzer Maximum, but there may be events during ascent that can be attributed to ultra-high energy air showers.

Studying radiation dose is not only important for safety during spaceflight but is also important for safety during commercial airline flights. Airplanes fly in the portion of the troposphere where air showers are at their peak in terms of particle density. As a consequence, passengers are exposed to relatively high doses of radiation. At these altitudes, neutrons contribute significantly to the overall radiation composition.

The MiniPIX [11] is a silicon-based particle detector integrated with a TimePIX [12] chip. The device is a result of the MediPIX Collaboration at CERN [13]. When an energetic particle is incident upon the sensor, energy is deposited in the detector, and the resulting data is recorded. For more detail regarding the functionality of the MiniPIX, refer to the previous flight report [2]. The MiniPIX's sensor can only detect charged particles, meaning it is unable to directly detect a neutron. However, through the use of a scintillator, the neutron can interact with the scintillator and produce a specific signature of charged particles which can be detected by the MiniPIX. An example can be seen from Uher et al. [14], who use a lithium-based scintillator to detect neutrons using a silicon-based detector. The reaction is

$$^{6}\mathrm{Li}^{+} + \mathrm{n} \longrightarrow {}^{3}\mathrm{H}^{+}\,\alpha(4.78\,\mathrm{MeV})$$

This iteration of the SORA payload attempted a similar procedure to measure neutrons but with the use of a boron loaded plastic scintillator [8]. The scintillator has a 5% boron loading and covered exactly half of the MiniPIX detector. The reaction between Boron-10 nucleus and a thermal neutron is

$$^{10}\mathrm{B} + \mathrm{n} \longrightarrow {}^{7}\mathrm{Li} + {}^{4}\mathrm{He} + \gamma(480\,\mathrm{keV})$$

according to Pawelczak et al [9]. This particular scintillator was chosen due to its relatively large reaction cross-section for thermal neutron capture and its emission of light charged particles in the thermal neutron capture reaction [9]. The larger cross-section increases the probability that the neutron will produce particles which can then be detected by the MiniPIX.

2. SORA PAYLOAD DESCRIPTION

With the successful completion of the first flight of SORA in 2017, the UH team decided to use the same materials with improved construction methods to build SORA 2.0. The design was optimized this year to use all the space available on the 2018 flight as shown on figure 2. The outer shell is KYDEX, a composite made of PVC and acrylic. KYDEX was initially chosen due to its properties. It is hydrophobic, UV resistant, and can withstand a wide range of conditions. It has a tensile strength of 6100 PSI and an impact strength of 15.00 ft.-lbs./in. The bolts used on the payload mainly were iron bolts with a weather-resistant coating. Brackets and other wall-mounting parts were nickel plated off-the-shelf parts.

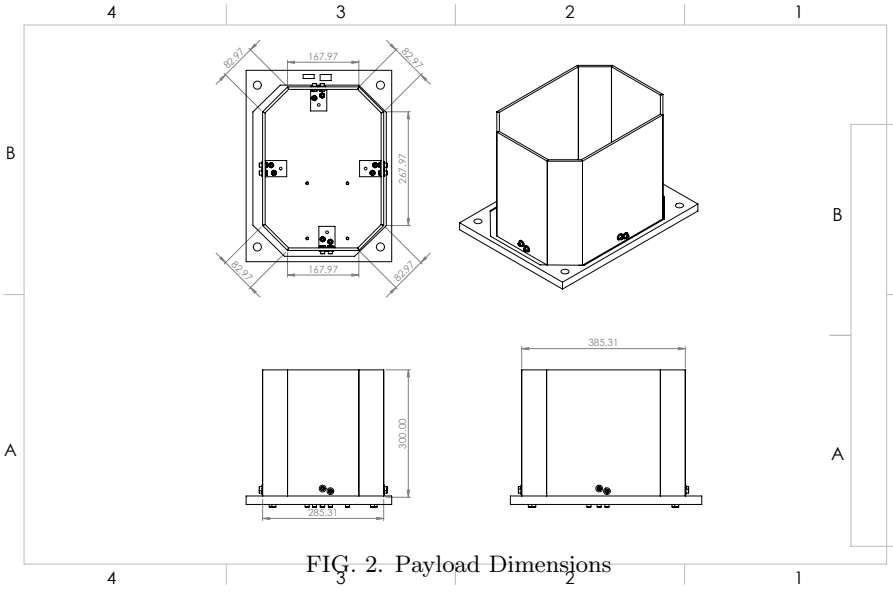

FIG. 2. Payload Dimensions

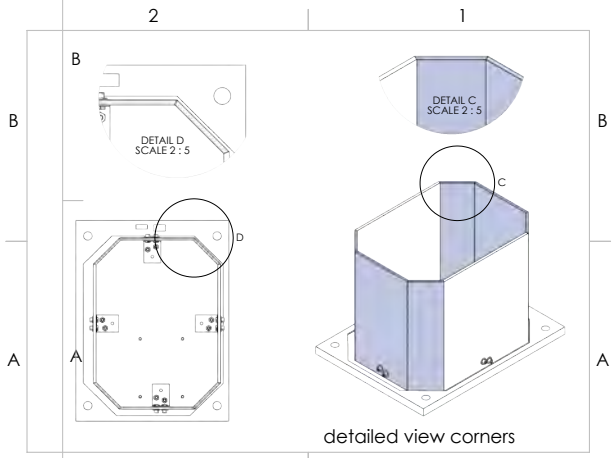

FIG. 3. Payload Corners

The outer shell was machine cut to our specified dimensions, including the corners so all the walls would sit flush against each other as seen in figure 3. This design allowed the team to fully take advantage of every inch of space provided on the flight. The biggest difference this year when compared to the 2017 flight is

that the payload shell encompasses all the systems. There are no external systems and this allowed the team to rearrange experiments in a more efficient manner. The overall system organization was kept simple. As shown in figures 4 and 5, the payload carried a full load of scientific equipment. The astrobiology system and the radiation MiniPIX system required specific positions as shown in figure 4. This was due to certain mechanical movements and ease of access to devices. The rest of the electronics were positioned as close as possible to the cable access ports that HASP provided on the payload plate.

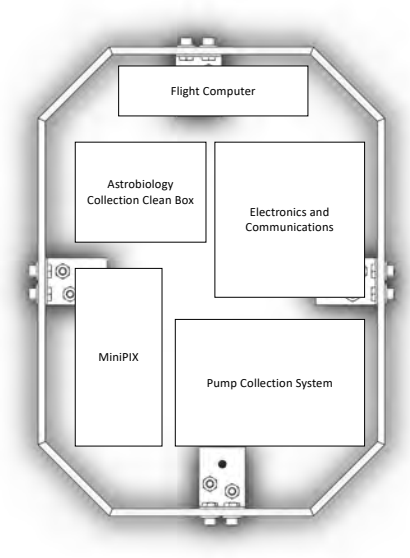

FIG. 4. Payload Sections and Space

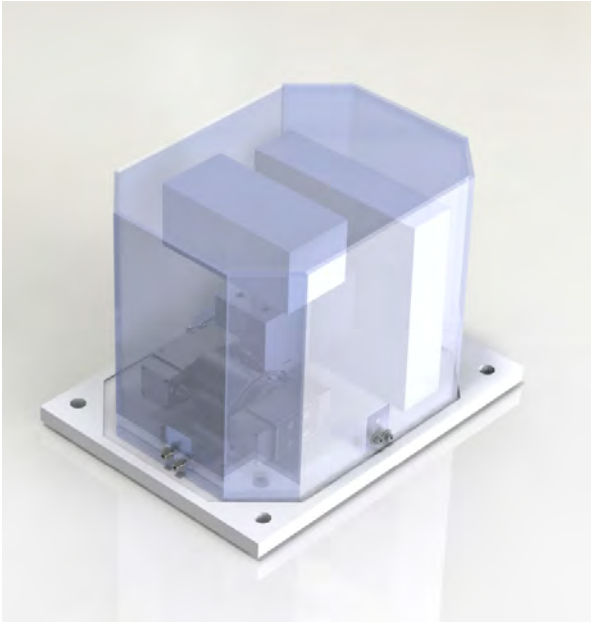

FIG. 5. Payload rendering with final flight configuration

2.1. Astrobiology System Design

The collection assembly was designed as a two-compartment structure, with one experimental collection and one control container, one pump, tubing to connect the components, and two solenoids. The clean box and containers were machined from impact-resistant ultra-high-molecular-weight polyethylene [10]. The control container was connected to a solenoid that remained closed until post-flight sanitation procedures were performed. The experimental sample collection container was connected to a vacuum pump located outside of the clean box structure. Once float altitude was reached, the solenoid connected to the experimental sample collection container was opened and the pump was powered on; allowing air to flow through the tubing exposed to the atmosphere to the collection container. Each container held approximately 2 mL of a 15% sterile glycerol solution. A 316 Stainless Steel 1/4" NPT Vent to Atmosphere Vitron Seal Valve was embedded in each of the compartments, to accommodate for the pressure changes that occurred with the variations in altitude over the course of the flight. The clean box displaying the collection containers and exhaust openings and a 3D rendering of the pump are shown in figure 6 below; the assembled astrobiology collection system is shown in figure 7 below.

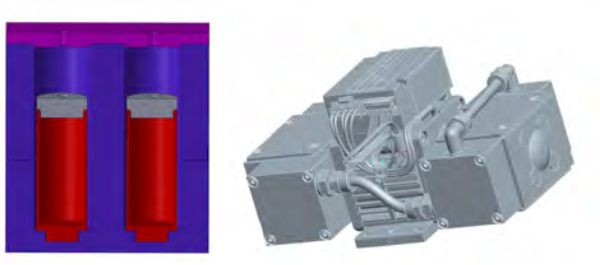

FIG. 6. Clean Box with Containers (left) and Pump (right).

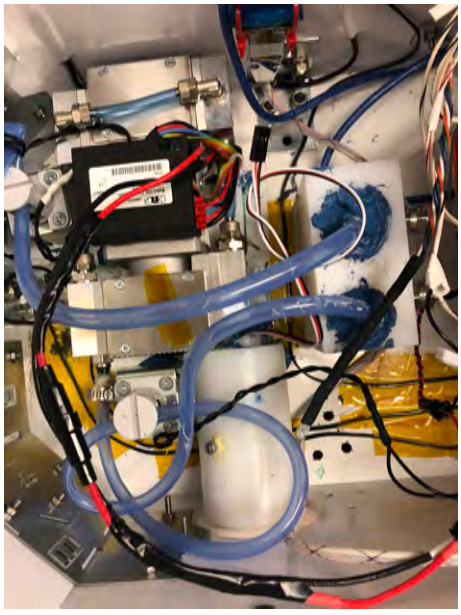

FIG. 7. Assembled Astrobiology Collection System.

2.2. Radiation Monitoring System Design

The Raspberry Pi 3 (RPI) has proven to operate at float altitudes both from the previous SORA flight and other HASP payloads from previous years. The RPI was chosen again to host the control and analysis software. Similarly to the 2017 SORA flight, both TimePIX devices were interfaced with the RPI via USB and controlled via the PyPixet library developed at CERN by Daniel Turcek. The major difference for the 2018 SORA flight is that the software was redesigned to support an arbitrary number of TimePIX devices to record data at the same time. This means that multiple TimePIX detector experiments could be run concurrently without adding another control system. Another major difference is that the detectors could be configured directly from the serial uplink and collected data could be downlinked in real-time. This allowed data from the detector to be analyzed and plotted in real-time by our mission control team.

The control and analysis software was written entirely in Python and operated directly on top of the default Raspbian image. The PyPixet software blocks when exposing the detector for collection. Therefore both detectors had to collect data in their own threads to allow the main thread to process uplink commands and control other systems. Data from each of these threads was then placed onto a queue where the main thread could periodically check if there was data ready to be processed. When a frame from one of the detectors was ready to be processed the main thread performed the analysis and then downlinked the results. Consequently, downlink speed was directly tied to shutter speed. An overview of the software design is shown in figure 8.

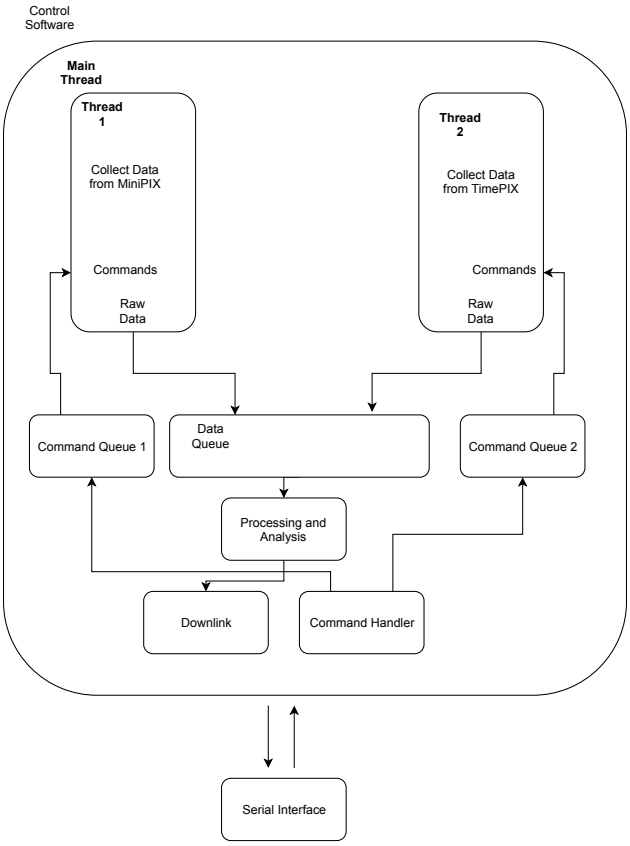

FIG. 8. Software design for the radiation control systems.

2.3. Telemetry

All telemetry was handled via the RPI. The DB9 interface from the HASP Large Payload plate was converted to a RS-232 female plug. A Male RS-232 to Male USB was used to connect it to a USB port of the RPI. The downlink data packets were written to describe the radiation data. The uplink commands were sent to the RPi which delegated the work either to itself or the Arduino which was connected to the RPI via USB.

2.3.1. Downlink

Downlink data was packetized at a rate of 160 bits per second and described the data being read from the MiniPIX detector. In addition, downlinked packets were interrupted with command queue messages for command confirmation. Each packet contained data listed in the Table II.

TABLE II. Downlink Packet Data by Bytes

Description	**Bytes**
Start of Frame	4
Control Byte	1
Data Length	1
MiniPix Temperature	4
Raspberry Pi Temperature	4
Frame Counts	4
Frame Dose Rate	4
Frame Count	4
Device ID	4
UNIX Timestamp	4
Error Flags	2
Checksum	4
End of Frame	1
Total	40

Each datum is separated by commas and each packet is delimited by a new line. This made it easy to parse. Since all packets were provided via the LSU HASP website, a web crawler program was written to plot in real-time data sent by the payload. These plots helped monitor the status of the payload over the course of testing, integration, and flight. figure 9 below shows the four plots created by the real-time plotter.

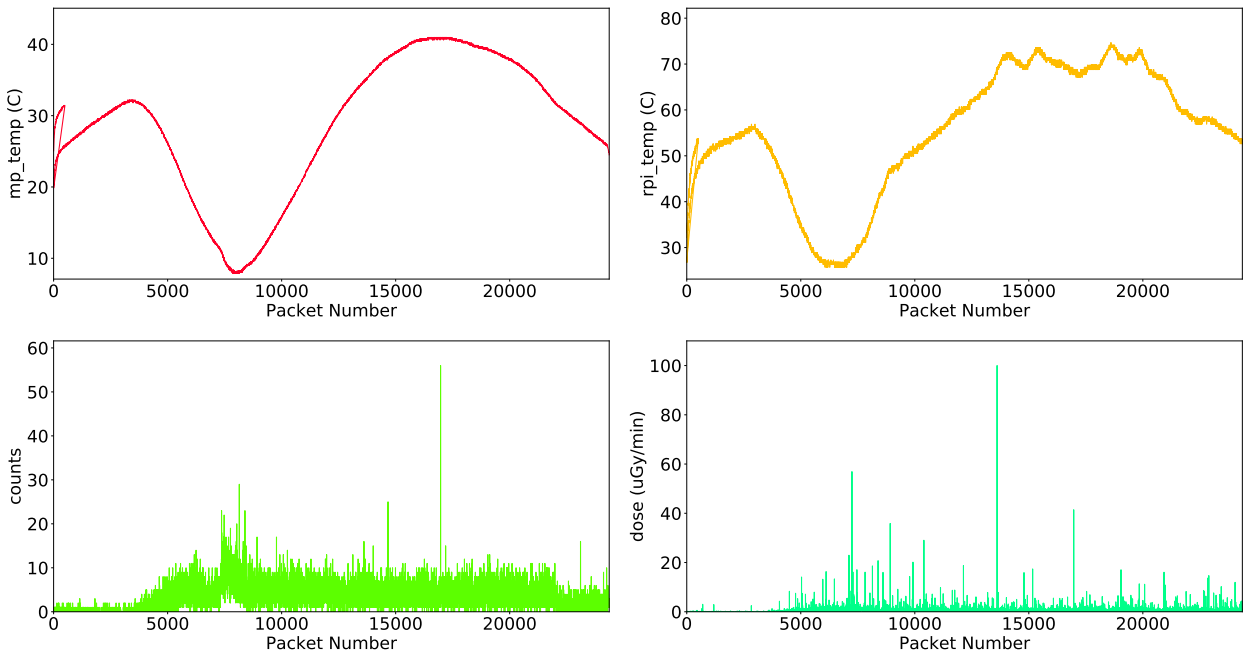

FIG. 9. Real-Time Plots from Payload 12 during flight

In the top left corner of figure 9 is the MiniPIX temperature in °C over packet ID. To its right is the RPI's temperature in degrees Celsius over packet ID. The bottom left corner plot depicts particle counts over its corresponding packet ID. Finally, to its right is the amount of radioactive dosage in µGy/min detected over packet ID. Listing 1 below denotes a sample of real data packets received during flight.

Listing 1. Sample of downlinked data packets ID: 15667 - 15670

```
1    ...
2    40.22,72.00,2.00,0.11214,15667,1,1532297412.36
3    40.22,72.00,5.00,0.52153,15668,1,1532297414.56
4    40.22,70.90,1.00,0.01183,15669,1,1532297416.85
5    40.22,71.40,4.00,0.99396,15670,1,1532297419.07
6    ...
```

No analog channels were required. All communication to and from the payload was done via HASP's integrated communication units.

2.3.2. Uplink

Uplink commands were used to start, end, and change parameters within our payload over the course of flight. Table III list the uplink commands, their functions, and a brief description of what they did. These commands were utilized about four time per hour. No on-board transmitters or receivers were used this year.

TABLE III. Table of All Uplink Commands Used During Flight

Command	Byte 1	Byte 2	Current Consumption (A)
Start Acquisition	0x01	-	0.47
End Acquisition	0x02	-	0.29
Change Shutter Rate	0x03	0x01 - 0xFF*	0.47
Change Acquisition Mode	0x04	0x01 or 0x02**	0.47
Astrobiology System On	0x05	-	1.8
Astrobiology System Off	0x06	-	0.47

* This parameter takes a hexadecimal integer that represents the number of seconds for each shutter of the MiniPix
** This parameter denotes which mode the MiniPix will operate in: 0x01 for fixed shutter rate, 0x02 for variable shutter rate

All commands were successfully sent, received, and processed during flight. Commands were confirmed through a change in current consumption or through a message from the command queue in the data packets.

3. METHODS

3.1. Astrobiology Methods

The clean box, the collection containers, and the tubing used to connect the components were all autoclaved for sterilization. A 70% ethanol solution was circulated through the pump to sterilize the internals. Everything used to assemble the system was then sprayed down with the ethanol solution before being placed inside a SterilGARD e3 Class II Biological Safety Cabinet. The 15% glycerol solution was pipetted into each container, the lids were sealed with epoxy, and tubing was inserted and epoxied into the holes in the container lid. Each lid had two holes, one that led to the inside of the clean box to allow for pressure to be released from inside the container and out-gassed through the valves embedded in the clean box. The other hole passed through the clean box lid to allow the tubing to connect to the pump, or pass through the solenoid only in the case of the control tubing. The clean box was apportioned to keep the experimental and control containers completely isolated from one another. Each container had their own pressure relief valve leading from their individual compartment within the clean box to the outside of the clean box. The lid to the clean box was sealed with epoxy and bolted closed, the tube from the control container was clamped by the dedicated control solenoid, while the tube from the experimental container was passed through the other solenoid and connected to the out-gassing nodule on the pump. The two holes in the clean box lid were sealed with epoxy and gasket maker to secure the tubing in place. The tube connected to the intake nodule on the pump was stabilized through an opening in the payload wall. The solenoid clamping the tubing to the experimental container remained closed until float conditions were achieved. Fluropore membrane filters (13 mm; 22 µm) were used to collect control samples in the labs where work was conducted and on the inside walls of the payload.

The payload was successfully retrieved on September 6, 2018. The intact payload was shipped to the University of Houston and received on September 12, 2018. The clean box and background samples were removed and placed in cold storage at −20 °C.

All equipment used in the filtration process was either autoclaved or taken from previously unopened sanitized packaging. The autoclaved, pre-sanitized items and the clean box were washed in a 70% ethanol solution before they were placed inside the Biological Safety Cabinet previously mentioned. The payload was successfully retrieved on September 6, 2018. The intact payload was shipped to the University of Houston and received on September 12, 2018. The clean box and background samples were removed and placed in cold storage at −20 °C. All equipment used in the filtration process was either autoclaved or taken from previously unopened sanitized packaging. The autoclaved, pre-sanitized items and the clean box were washed in a 70% ethanol solution before they were placed inside the Biological Safety Cabinet previously mentioned.

The control sample collection solution was vacuum filtered through a Fluropore membrane filter (13 mm; 22 µm) to collect specimens on the filter surface. The experimental sample collection container was thoroughly

swabbed with a Fluropore membrane filter as the glycerol coated the inside of the container and the full sample could not be pipetted out of the container to pass through the vacuum and onto the filter. All filters were processed using the DNeasy PowerWater Kit by QIAGEN [17] in preparation for 16S ribosomal RNA sequencing.

3.2. Cosmic Radiation Methods

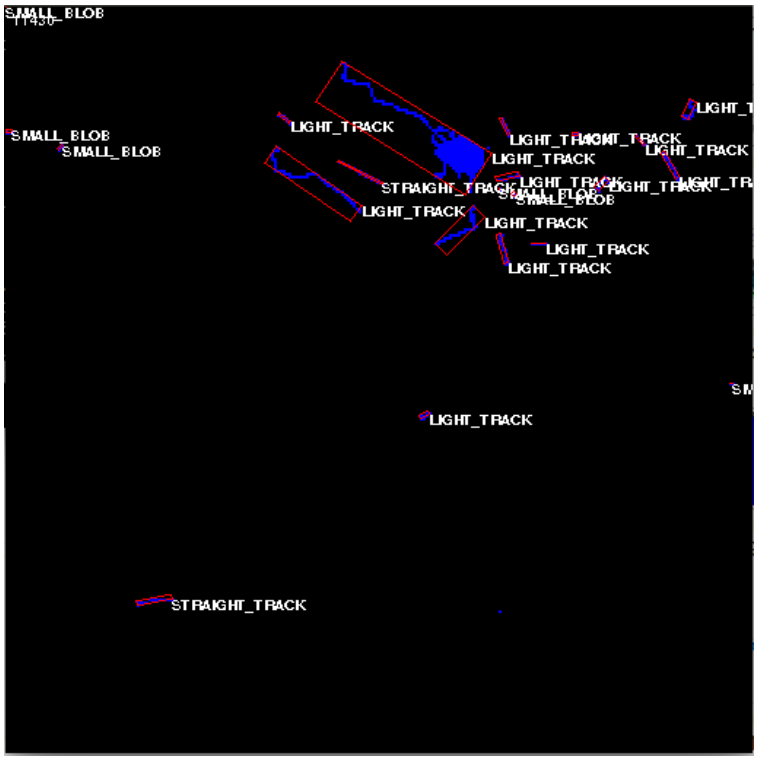

FIG. 10. Bounding boxes calculated for a frame of flight data.

The output format of TimePIX devices provides a great deal of flexibility in terms of data analysis. The data can provide both a simple absorbed dose from ionizing radiation as well as insight into more detailed dosimetric endpoints like dose equivalent. Additionally a clustering procedure can be performed to analyze individual particle interactions in the detector based on their morphological properties.

Since energy deposition can be determined on a per pixel basis, absorbed energy is calculated via a simple summation across all pixels in a frame of data after applying a standard calibration procedure outlined by Jakubek et al. [20]. With knowledge of the mass of the detector volume you can then calculate a dose by dividing the deposited energy by the detector mass. Thus a simple dose in silicon is calculated as

$$D_{Si} = \frac{E}{M_d}$$

To analyze the data on a per track basis first, a clustering procedure has to be performed to separate the data in a frame into individual tracks. This can be accomplished by applying a simple algorithm used in image processing called Flood-Fill; whereby contiguous nonzero pixels are recursively filled and grouped together into clusters. Then, after calculating a minimum area bounding box and linear least squares fit a

track length is calculated by determining where the least square fit line intersects with the bounding box. Additionally, an azimuth angle can be determined relative to the detector orientation and a density can be calculated by dividing the number of pixels in a cluster by the area of the bounding box. A simple visual example of these calculations is shown in figure 11 and a visualization of the bounding boxes calculated for a frame of data is shown in figure 10.

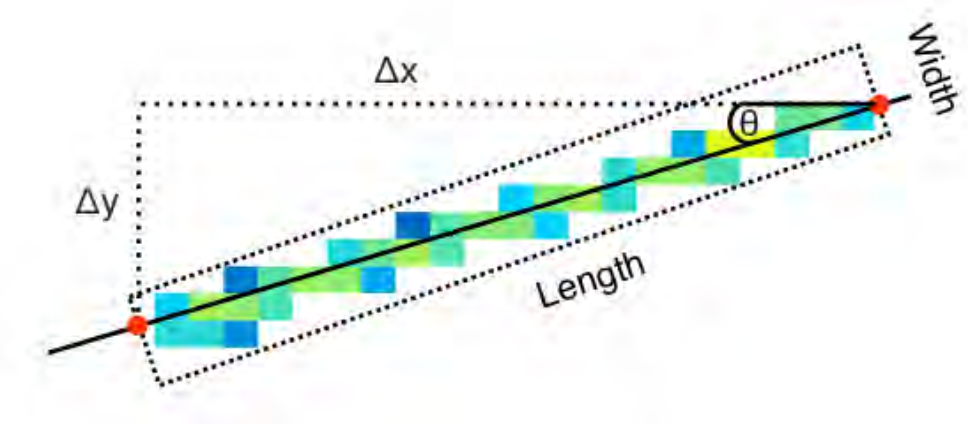

FIG. 11. Track parameter calculation.[18]

Given the track length calculated from the fit line and the bounding box, a three-dimensional track through the detector can be constructed by using simple trigonometry. Given the sensor thickness T and the projected track length L_p the length of the track through the detector L can be calculated by

$$L = \sqrt{L_p^2 + T^2}$$

With a true track length calculated one can then calculate the linear energy transfer (LET) of a track by dividing the total energy deposited in a cluster E by the track length L. LET is an important reference as it provides a standard measurement for a track that is independent of the angle of incidence for an incident particle. While not discussed in detail in this report LET is also the quantity that is used in calculating dose equivalent in flesh.

$$LET_{Si} = \frac{E}{L}$$

Another standard technique used when analyzing TimePIX data is sorting clusters in the data based on their morphological characteristics. After clustering, additional processing is applied to calculate individual track parameters. These parameters can then be placed into a simple sorting algorithm that assigns them labels based roughly on their characteristics. The idea behind this morphological analysis is that information regarding the origin of the particle that made the track can be elucidated on the principle that similar types of particles will create similar shaped tracks in the detector. Based on a tracks density, pixel count, inner pixel count and ratio between the bounding box's length and width a track is sorted as either a small blob, medium blob, heavy blob, light track, straight track or heavy track. The specifics of the algorithm are defined in figure 12.

Type	Inner Pixels	Length/ Width Ratio	Other Criteria	Example Tracks
Small Blob	0	-	1 or 2 Pixels, 3 if L shape, 4 is square	
Heavy Track	> 4	> 1.25	Not S.Blob Density > 0.3	
Heavy Blob	> 4	< 1.25	Not H.Track Density > 0.5	
Medium Blob	> 1	< 1.25	Not H.Blob Density > 0.5	
Straight Track	0	> 8	Not M.Blob Minor axis < 3 pixels	
Light Track	-	-	Not S.Track	

FIG. 12. Track morphology algorithm [19].

While the track morphology does not provide a hard and fast classification, a rough idea of the origin of a track in a mixed radiation field can be determined. Possible origins of track morphology are shown in figure 13.

Cluster Type	Possible Origin
Small Blob	Low energy short range particle/interaction, i.e. x-ray photoelectron or neutron elastic scattering [57]. Number of pixel hits determined by position of interaction in pixel (see section 2.4.3).
Heavy Track	High energy ($\gtrsim 20\,\mathrm{MeV}$), heavy ($Z \geqslant 1$) charged particle e.g, proton $> 20\,\mathrm{MeV}$ or alpha $> 100\,\mathrm{MeV}$.
Heavy Blob	High energy ($\gtrsim 2\,\mathrm{MeV}$), short range (few µm in Si) particle.
Medium Blob	Fast charged particle at high angle of incidence, very slow charged particle ($\lesssim 2\,\mathrm{MeV}$) or fast neutron interaction (see section 3.5.3 or [57]).
Straight Track	Light minimum ionizing particle (muon, fast proton, pion etc).
Light Track	Multiple scatterer (electron, positron $\gtrsim 100\,\mathrm{keV}$).

FIG. 13. Possible physical origins of cluster morphology [18].

4. RESULTS

4.1. Astrobiology Results

One goal of this project was to confirm our results from last year. To that end we selected the same 926wF ("AAACTYAAAKGAATTGRCGG") and 1392R ("ACGGGCGGTGTGTRC***") primers for the sequencing procedure [2]. These primers are designed to amplify 16S RNA from bacterial, archaeal and eukaryotic "universal" samples. The samples were sent to the University of Houston Seq-N-Edit Core [15] and processed using the QIAseq 16S/ITS protocols [16]. The samples were quantified using a Qubit Fluorometer; the results yielded 28 of the 25 pg/µL-minimum in the experimental sample only. DNA was not detectable in the control samples. The control samples were pooled. Both the pooled control samples and the experimental sample were concentrated using a bead extraction technique. The yield was 248 pg/µL in the experimental sample and 141 pg/µL in the pooled control background sample. Finally, a midpoint quality control check was performed where it was determined that, while DNA was detectable, the integrity was too low to merit proceeding to the next phase involving several thousand dollars' worth of materials.

4.2. Cosmic Radiation Results

A total of 16,376 frames were collected during flight and recovered successfully from the payload. Shown in figure 14 are a sample of tracks collected at float. The image shown in figure 14A in the upper left likely shows an interaction from a heavy ion while the rest of the tracks show a sampling of light and straight tracks.

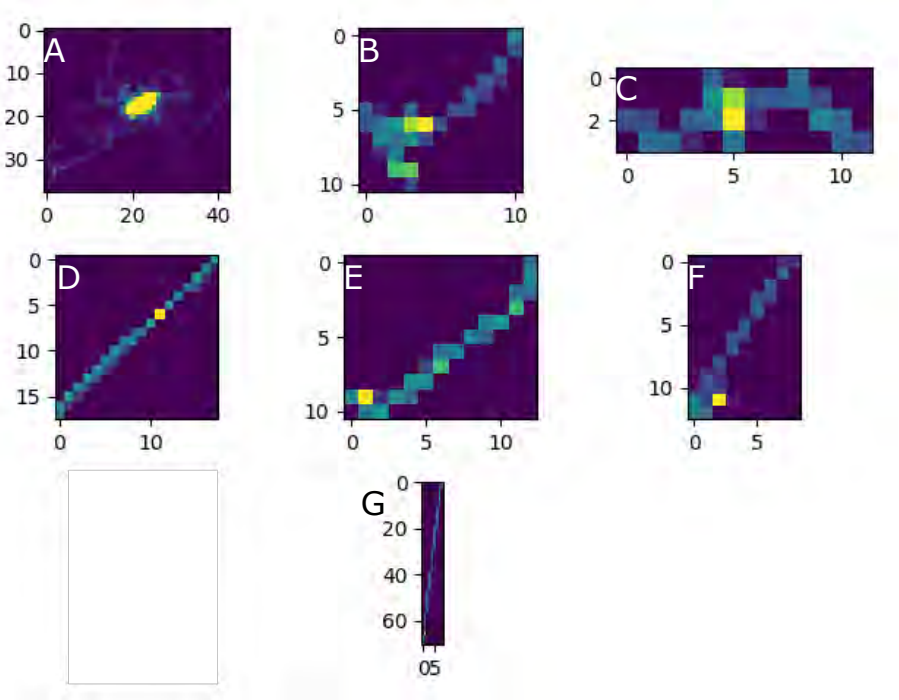

FIG. 14. Tracks collected at float.

Shown in figure 15 (a) is the LET distribution for the entire population of tracks collected at float while 15 (b) shows the LET distribution split up by track classification.

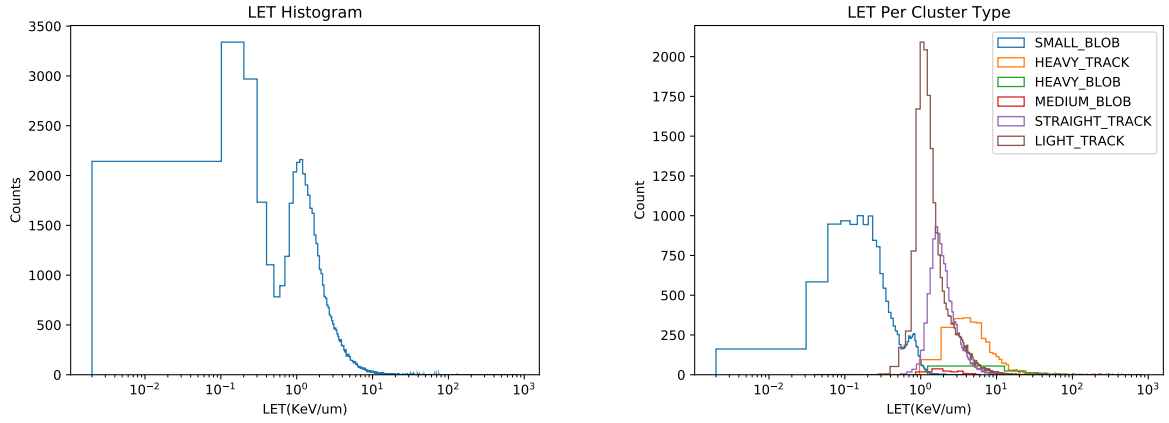

(a)LET histogram from data collected during the duration of the flight.

(b)LET histogram from each cluster type.

FIG. 15. LET distributions data from Flight

Shown in figure 16 is a comparison of the count rate for the SORA 2017 and 2018 flight. The shape of the data is nearly identical however one can observe that the 2018 flight has a higher variability and is slightly less homogeneous when compared to the 2017 data. The overall variability is due to a faster frame rate. The period of decreased variability that occurs just after the peak is due to a test of the ability to dynamically modify the frame rate via uplink commands. Another significant feature of the data is that the 2018 flight appears to be shifted upwards by approximately two counts per second when compared to the 2017 data. This would seem to suggest a higher flux during the 2018 flight.

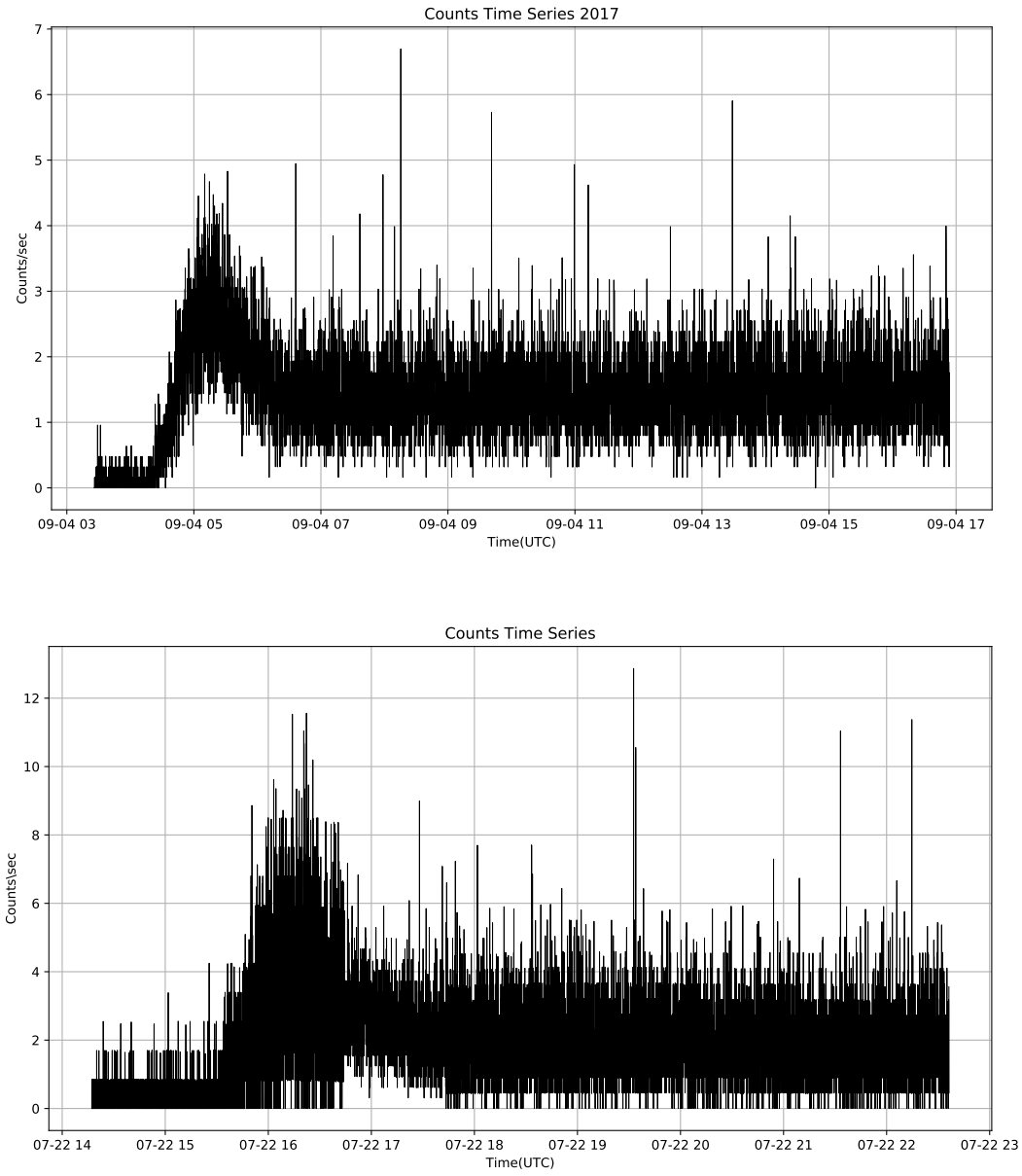

(b)Counts from data collected during the 2018 flight.

FIG. 16. Cluster counts data from Flights 2018 and 2017

5. DISCUSSION

FIG. 17. Final payload integrated and ready for flight

SORA 2.0 was safely recovered after landfall. Thanks to the outer shell and build quality, all payload subsystems showed no damage. The plastic insulation and reinforced openings aided in maintaining a stable operating temperature within the payload walls. Data and sample integrity both were achieved successfully. As seen in figure 9, data was downlinked without faults or missing datum. For astrobiology, samples were recovered safely and sent to be analyzed. The only change to the structure that provided a significant advantage during flight was adding duct tape to the corners of the payload walls. As seen in figure 17, the tape covers the corners which allowed for a passive but effective way to manage internal temperature.

Overall, the Kydex, flight-proven outershell structure served its purpose once again. The impact protection, solid construction, and insulation properties of the shell allowed for uninterrupted experiments to take place in the harsh environments of the upper atmosphere.

5.1. Astrobiology Discussion

We were unable to obtain results from this year's samples. In our 2017 experiment, we had two samples for processing and it cost our team nearly $1,500 for RNA sequencing and analysis. This year we had almost a dozen samples, including our background samples, and could not afford to send them to RTL Genomics again. We were fortunate to partner with the Seq-N-Edit Core at the University of Houston, who sponsored the materials and researcher hours related to the DNA processing and preparation for 16S ribosomal RNA sequencing. A key difference in the DNA extraction step was the use of the Qiagen DNeasy Powerwater kit rather than the MoBio PowerWater kit [2]. The Qiagen kit is a new release and may not be as robust as the MoBio kit. A field representative from QIAGEN is scheduled to meet with Ian Wilson, in the UH Seq-N-Edit Core, during the week of December 3rd 2018 to discuss the kit and our results. Although we do not have definitive results at this time, we are hopeful that the field representative will provide additional insight on how best to tailor the DNA washing kit protocols for samples types such as ours going forward. It was suggested that we optimize our own set of protocols by collecting multiple ground samples and using the kit with various DNA extraction protocols until we find an optimal method. We have also decided to

pursue an altogether different mode of collection for next year in hopes of increasing the number of replicates and the surface area available for collection. If we can obtain a large enough sample-size we hope to culture the organisms collected in future experiments, in addition to sequencing the 16S rRNA. There is much to be learned from living cells that can survive under the float conditions to which our payload was subjected. If our results can be repeated and confirmed, it would also demonstrate that there are more organisms that are able to survive under our payloads flight conditions than previously documented and provide additional confirmation as to the existence of the currently documented organisms.

5.2. Radiation Discussion

By and large the most significant changes in the radiation system for SORA were technical in nature. This iteration of SORA saw vast improvements in the collection and analysis system. Most significant among these improvements were the ability to handle multiple detectors on a single RPI, the ability to analyze data in real time and the ability to configure device parameters such as the frame rate in real time via uplink commands.

The 2018 flight also provided an opportunity to compare data in similar conditions to our 2017 flight. While the composition of the data looked fairly similar in terms of LET distributions, the most striking difference observed was that of the detector count rate. The 2018 data showed a net increase of approximately 1-2 counts per second on average. This increase could potentially be explained by the addition of the scintillator coupled to the detector surface or simply by variation in the flux of cosmic radiation in the atmosphere.

The count difference provides a good platform for future missions during which the neutrons can be more closely examined as the solar cycle develops. Hathaway [6] has shown the direct relationship between the development of the solar cycle and the average neutron counts. By maintaining a similar detection technique for several years, the data should display a trend similar to that observed by Hathaway. Additionally, a larger array of MiniPIX devices would likely be required, as the active surface area of a single MiniPIX is rather small. In order to make a confident determination in a trend, a larger active surface area would be required to offset the natural small fluctuation in neutron density.

The MiniPIX and TimePIX detectors have proven to be robust and resilient towards large thermal fluctuations. However, during the course of integration testing in Palestine, TX, a failure was observed. During the cold cycle of the test a slow but steadily increasing number of counts was observed that is anomalous to what one would expect near the earths surface. The expected number of counts per second (CPS) should have been close to 3 CPS but the downlinked data was reporting values of over 300 CPS as shown in figure 18. A correlation analysis was performed and showed that there was no direct correlation between device counts and temperature. Additionally, this behavior was not observed on an identical detector used during the 2017 SORA flight [2].

After consulting with some of the members of the TimePIX collaboration at the University of Houston and NASA we were informed that they were unable to determine a concrete reason for the failure but did provide a couple of possible explanations. The first but least likely cause is that of a single event upset in the device causing the detector threshold to be lowered. TimePIX devices deployed on the International Space Station often experience this kind of behavior and consequently reload their configurations every few frames to prevent it. This is a remote possibility given the low levels of high energy particles near the earths surface. Another possibility is that the temperature changes caused a partial failure in the power supply and the RPI was unable to provide enough power to the detector. This is a more plausible explanation. However, given that the failure was not observed again, it is difficult to determine the cause.

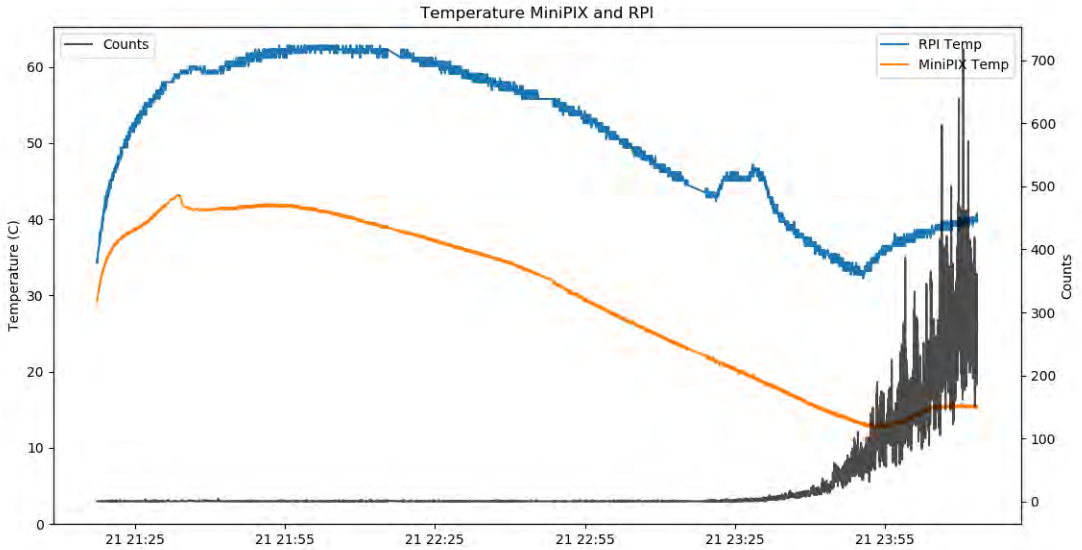

FIG. 18. Temperature of flight computer and detector and counts during integration testing in Palestine, TX.

6. CONCLUSION

Although DNA was detectable in our samples, we were unable to advance to the next phase in the process of RNA sequencing. We are hopeful that alterations to the DNA extraction protocols will allow for more definitive results in the future. Additionally, a new collection assembly designed to maximize the experimental sample volume is one of the main objectives of next year's flight. There is much to be learned from living cells that can survive under the float conditions our payload was subjected to at altitude. Genomic, proteomic, and metabolomics comparisons between the high-altitude atmospheric samples and near/at surface samples may yield useful insight into organic radiation shielding and adaptations for survival in extreme conditions. Further missions would help expand on discovering more about these organisms.

The MiniPIX gathered a wealth of information, with a total of 16,376 frames collected during flight. The radiation data is still being analyzed. There was a significant increase in particle counts this year, which may be attributed to the addition of the plastic scintillator. The MiniPIX system can be expanded further by the addition of more MiniPIX devices, which would yield a larger volume of data. This year's mission provided a foundation for future flights through the addition of a robust and developed flight computer. Furthermore, the adjustable MiniPIX system via uplink commands expands the functionality of the payload.

Appendix A COLLABORATION DEMOGRAPHICAL INFORMATION

Name	Role	Student Status	Race	Ethnicity	Gender	Disabled
Andrew L. Renshaw	Faculty Mentor	Faculty	White	N/A	Male	No
Samuel A. Garcia Morelos	Project Leader	Post-Bachlor	White	Hispanic	Male	No
Fre'Etta Brooks	Astrobiology Coordinator	Post-Bachelor	Black	N/A	Female	No
Steven Oliver	Radiation Coordinator	Post-Bachelor	White	N/A	Male	No
Reed Masek	Command and Data Handling	Undergrad	White	N/A	Male	No
Andrew Walker	Lead Programmer	Post-Bachelor	White	Hispanic	Male	No
Kevin Portillo	Command and Data Handling	Undergrad	White	Hispanic	Male	No
Jimish Patel	Astrobiology	Undergrad	Asian	Indian	Male	No
Stuart George	MiniPIX Expert	Post-Graduate	White	N/A	Male	No
Donna Pattison	Faculty Mentor	Faculty	White	N/A	Female	No
Ian Wilson	Microbiology Expert	Graduate Student	White	N/A	Male	No
Preethi Gunaratne	Faculty Advisor	Faculty	Asian	Indian	Female	No

[1] High Altitude Student Platform Flight Data http://laspace.lsu.edu/hasp/Flightinfo.php
[2] S.A. Garcia Morelos, F.Brooks, S.Oliver, A.Walker, K.D. Portillo, R.B. Masek, D.Mroczek, D.Pena, J.Juarez, A.Cruz, D. Henandez, S.George, D. Pattison, A.L.Renshaw. *SORA 2017 Mission Webpage*, http://laspace.lsu.edu/hasp/groups/Payload.php?py=2017&pn=10.
[3] Extremophiles http://www.nytimes.com/2013/02/07/science/living-bacteria-found-deep-under-antarctic-ice-scientists-say.html.
[4] https://helios.gsfc.nasa.gov/gcr.html
[5] Regener E. & Pfotzer G., *Vertical Intensity of Cosmic Rays by Threefold Coincidences in the Stratosphere.*, Nature 136, 718-719, (1935).
[6] Hathaway, D. H. (2015). The Solar Cycle. Living Reviews, 12. doi:10.1007/lrsp-2015-4
[7] Schröder, F. G. (2017). Radio detection of cosmic-ray air showers and high-energy neutrinos. Progress in Particle and Nuclear Physics, 93, 1-68. doi:10.1016/j.ppnp.2016.12.002
[8] EJ-254 Boron Loaded Plastic Scintillator https://eljentechnology.com/images/products/data_sheets/EJ-254.pdf.
[9] Pawełczak, I., Glenn, A., Martinez, H., Carman, M., Zaitseva, N., & Payne, S. (2014). Boron-loaded plastic scintillator with neutron-γ pulse shape discrimination capability. Nuclear Instruments and Methods in Physics Research Section A: Accelerators, Spectrometers, Detectors and Associated Equipment, 751, 62-69. doi:10.1016/j.nima.2014.03.027
[10] Clean box material https://www.mcmaster.com/#uhmw-polyethylene/=1aijn1p.
[11] MiniPIX - Miniaturized Portable USB Photon Counting Camera. (n.d.). Retrieved February 02, 2017, from http://advacam.com/camera/minipix.
[12] Timepix chip at https://medipix.web.cern.ch/technology-chip/timepix3-chip
[13] Medipix collaboration at https://medipix.web.cern.ch/.
[14] Uher, J., Frojdh, C., Holy, T., Jakubek, J., Petersson, S., Pospisif, S., . . . Stekl, I. (2007). Silicon Detectors for Neutron Imaging. AIP Conference Proceedings. doi:10.1063/1.2825756
[15] UH Seq-N-Edit Core at http://seqnedit.nsm.uh.edu/.
[16] QIAseq Protocols at https://www.qiagen.com/us/resources/resourcedetail?id=07fa061e-c9e8-44b9-9b09-6af351e632cd&lang=en.
[17] PowerWater Kit Protocols at https://www.qiagen.com/us/resources/resourcedetail?id=bb731482-874b-4241-8cf4-c15054e3a4bf&lang=en.
[18] George, S., *Dosimetric Applications of Hybrid Pixel Detectors*, University of Wollongong, Australia, 2015.
[19] Reprinted from *Dosimetric Applications of Hybrid Pixel Detectors* by Stuart George, 2015, Mixed Field Measurements and Cluster Formation with Timepix,52.
[20] Jan Jakubek, *Precise energy calibration of pixel detector working in time-over-threshold mode* Institute of Experimental and Applied Physics, Czech Technical University in Prague, Czech Republic, 2011.